$(OH)(OH_2)_n]_2[SiAlO_4]_6$ with $n > 1$ proposed by several authors could be identified.

2. Hydrothermal reaction of kaolinite and concentrated aqueous NaOH solution under various conditions yields basic hydrosodalite $[Na_4(O_2H_3)]_2[SiAlO_4]_6$ as the primary synthesis product. However, the latter may be partly transformed into nonbasic $[Na_3\square(OH_2)_4]_2[SiAlO_4]_6$ sodalite due to exchange of intracage NaOH against H_2O during washing the crude product with water to remove excess NaOH from the outer surface of the crystallites. The extent of intracage $NaOH/H_2O$ exchange depends on the washing conditions and the specific surface (crystallite size) of the synthesis products. The extraction of NaOH from the cages by H_2O washing is considerably reduced only for large single crystal products (crystal size 0.5-1 mm) prepared under high-pressure/high-temperature conditions of hydrothermal synthesis according to route A.

3. Basic hydrosodalite hydrates $[Na_4(OH)(OH_2)_n]_2[SiAlO_4]_6$ with $n > 1$ frequently described in the literature do not exist but are mixtures of basic $[Na_4(O_2H_3)]_2[SiAlO_4]_6$ and nonbasic $[Na_3\square(OH_2)_4]_2[SiAlO_4]_6$ sodalites. These mixtures are formed by the above-mentioned intracage $NaOH/H_2O$ exchange during the washing process of the primary $[Na_4(O_2H_3)]_2[SiAlO_4]_6$ synthesis product.

4. The dehydrated hydroxysodalite $[Na_4(OH)]_2[SiAlO_4]_6$ cannot be rehydrated to the $[Na_4(O_2H_3)]_2[SiAlO_4]_6$ composition even in excess of water at higher temperature. In contrast, the anhydrous nonbasic sodalite $[Na_3\square]_2[SiAlO_4]_6$ is highly hydrophilic and rehydrates with water to the $[Na_3\square(OH_2)_4]_2[SiAlO_4]_6$ sodalite via an intermediate phase of composition $[Na_3\square(OH_2)_2]_2[SiAlO_4]_6$.

Acknowledgment. We acknowledge the Alfried Krupp von Bohlen und Halbach-Stiftung, Essen-Bredeney, and the Bundesminister für Forschung und Technologie, Bonn-Bad Godesberg, for financial support of this work. We thank Mr. Wessiken, ETH Zürich, for the scanning electron micrographs of Figure 5, Dr. Ch. Buhl for valuable discussions, and Mr. G. Wildermuth and Mr. A. Straub for technical assistance in the thermoanalytical and X-ray diffraction experiments. We are also grateful to Bruker Analytische Messtechnik, Karlsruhe, for the possibility to measure the MAS-NMR spectra and to Dr. M. Smith and Dr. H. Foerster for assistance in these measurements and helpful discussions.

Structure of the Heme *o* Prosthetic Group from the Terminal Quinol Oxidase of *Escherichia coli*

W. Wu,[†] C. K. Chang,*,[†] C. Varotsis,[†] G. T. Babcock,*,[†] A. Puustinen,[‡] and M. Wikström*,[‡]

Contribution from the Department of Chemistry, Michigan State University, East Lansing, Michigan 48824-1322, and Helsinki Bioenergetics Group, Department of Medical Chemistry, University of Helsinki, Siltavuorenpenger 10A, SF-00170 Helsinki, Finland.
Received August 9, 1991

Abstract: The structure of the heme *o* prosthetic group of *Escherichia coli* quinol oxidase (cytochrome *o* oxidase) has been unambiguously determined by preparation and characterization of its iron-free derivative porphyrin *o* dimethyl ester, or dimethyl 2,7,12,18-tetramethyl-3-[(4*E*,8*E*)-1-hydroxy-5,9,13-trimethyltetradeca-4,8,12-trienyl]-8-vinylporphine-13,17-dipropionate. The identity of this natural porphyrin dimethyl ester was established by ^1H NMR, MS, IR, and RR spectroscopies as well as by comparisons with model compounds and the closely related porphyrin *a* dimethyl ester. The reliability of the structure determination was further strengthened by the isolation and characterization of the acetylated and dehydrated derivatives of porphyrin *o*.

Aerobically grown *Escherichia coli* express two membrane-bound, multi-heme respiratory proteins: cytochrome *o* oxidase at high O_2 concentration and cytochrome *d* oxidase at low O_2 level.[1-4] Both are linked to hydrogenases via a ubiquinone pool. Cytochrome *d* oxidase has two b-type hemes and an oxygen-binding d-type heme which catalyzes O_2 reduction to H_2O. The structure of the heme *d* prosthetic group was recently established by spectral characterizations[5] and by total synthesis.[6] In contrast, cytochrome *o* oxidase has two hemes and one Cu ion[7] where one heme and the copper center form a binuclear metal catalytic site[3] for binding and reduction of O_2. Therefore, this enzyme bears a strong resemblance to mitochondrial aa_3 cytochrome oxidase, which is also exhibited by the primary protein structure.[2] Since the absorption spectrum of the cytochrome *o* heme group is roughly similar to b-type hemes, its structure had been assumed to be that of protoheme. Recently, Puustinen and Wikström[8] have suggested that the hemes of cytochrome *o* are of a novel kind, for which they proposed the name heme *o*. The structure of heme *o* (**1a**) was proposed to be heme *a* like, containing a 17-carbon farnesylhydroxyethyl side chain but with a methyl residue replacing the formyl group at pyrrole ring D. This proposed

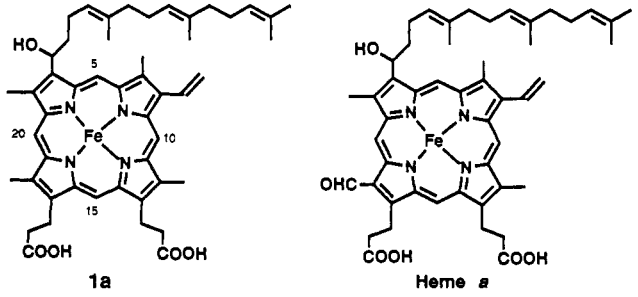

structure was based on the following observations: (1) Chromatographic analysis of the extracted heme *o* revealed that it is

[†] Michigan State University.
[‡] University of Helsinki.

(1) Anraku, Y.; Gennis, R. B. *Trends Biochem. Sci.* **1987**, *12*, 262-266.
(2) Chepuri, V.; Lemieux, L.; Au, C. C-T.; Gennis, R. B. *J. Biol. Chem.* **1990**, *265*, 11185-11192.
(3) (a) Salerno, J. C.; Bolgiano, B.; Poole, R. K.; Gennis, R. B.; Ingledew, W. J. *J. Biol. Chem.* **1990**, *265*, 4364-4368. (b) Bolgiano, B.; Salmon, I.; Ingledew, W. J.; Poole, R. K. *Biochem. J.* **1991**, *274*, 723-730.
(4) Miller, M. J.; Gennis, R. B. *J. Biol. Chem.* **1983**, *258*, 9159-9165.
(5) (a) Timkovich, R.; Cork, M. S.; Gennis, R. G.; Johnson, P. Y. *J. Am. Chem. Soc.* **1985**, *107*, 6069-6075. (b) Andersson, L. A.; Sotiriou, C.; Chang, C. K.; Loehr, T. M. *J. Am. Chem. Soc.* **1987**, *109*, 258-264.
(6) Sotiriou, C.; Chang, C. K. *J. Am. Chem. Soc.* **1988**, *110*, 2264-2270.

0002-7863/92/1514-1182$03.00/0

highly hydrophobic relative to protoheme. Its retention time was even longer than that of heme *a* in a reverse-phase HPLC chromatographic column. (2) The pyridine hemochrome spectrum of heme *o* is 4 nm blue shifted in comparison with protoheme, suggesting that a saturated side chain replaces one of the two vinyl groups of protoheme. Furthermore, unlike heme, *a*, it does not have an extensive red shift of the native and pyridine hemochrome spectra, which arise for heme *a* from the diagonally arranged vinyl and formyl groups. (3) Fast atom bombardment mass spectrometry of heme *o* gave a molecular mass of 839 Da, which is 14 mass units less than that of heme *a*, corresponding to a methyl group in place of the formyl group. While these arguments for the new heme *o* structure are rational and attractive, more direct spectroscopic evidence is needed to establish its validity. This paper reports the experiments and evidence that lead to the unambiguous determination of the heme *o* structure.

Experimental Section

1. Materials and Methods. General Procedure. FAB (fast atom bombardment) mass spectra were recorded on a JEOL HX-110 HF double focusing mass spectrometer operating in the positive ion detection mode. The samples were dissolved in methylene chloride as cosolvent, and 1 μL of the solution was mixed with 2 μL of NBA (*m*-nitrobenzyl alcohol) matrix on the probe tip for spectral acquisition. The samples were bombarded by a beam of neutral Xe atoms (6 kV), and the accelerating voltage was 10 kV. UV–visible spectra were measured on a Cary 219, a Shimadzu 160, or a Perkin-Elmer lambda-5 spectrophotometer, with samples dissolved in dichloromethane. IR spectra were recorded on a Nicolet FTIR-42 spectrometer, the samples were prepared as a thin film on NaCl plates, and the wavenumbers are reported with an accuracy of ±2 cm^{-1}. ^1H NMR spectra were recorded on Varian Gemini-300 or VXR-500 spectrometers, in "100%" chloroform-*d* (minimum 99.96 atom % D, Isotec Inc.) with the residual $CHCl_3$ as the internal standard set at 7.26 ppm. Resonance Raman spectra were obtained from 0.1–0.5 mM samples in CH_2Cl_2 solution in a cylindrical quartz spinning cell for heme *o*, and a jet cell[9a] for heme *a* at room temperature. The Raman equipment included a Spex 1459 illuminator, a Spex 1877 Triplemate with an EG&G Model 1421 diode array detector and an OMA III computer. An Innova 90 krypton ion laser system was used to provide an excitation wavelength of 406.7 nm, and the power incident on the sample was 20 mW. In all cases, the stability of the complex under study to the laser irradiation employed was confirmed by the observation that the UV–visible absorption spectra before and after the RR measurements were unchanged.

Preparative thin-layer chromatography (TLC) was performed on commercial Analtech plates (silica gel G, 20 × 20 cm, 1000 μm). After extraction of the separated bands, removal of solvents was carried out under reduced pressure on a Buchi Rotavapor at 30–40 °C. All solvents were freshly distilled before use. All manipulations were carried out under subdued light to avoid possible side reactions.

The chloride complex of ferric heme *a* was prepared by acetone/HCl extraction of isolated cytochrome oxidase from bovine heart.[9b] Ferric heme *o* was purified by HPLC after acetone/HCl extraction of membranes from *E. coli* strain RG 145.[8] Model porphyrins **4** and **5** were synthesized from partial dehydration of hematoporphyrin IX dimethyl ester according to a literature procedure.[10] Iron insertion of these two porphyrins was accomplished by using the $FeSO_4$/HOAc/pyridine method.[11a] Model porphyrin **6** was obtained by total synthesis as described previously.[12]

2. Preparation of Porphyrin *o* Dimethyl Ester 1b and Derivatives 2 and 3. The iron(III) heme *o* (2 mg, 2.3 μmol) was dissolved in 1 mL of pyridine and glacial acetic acid (20 mL, distilled from $FeSO_4$). The solution was purged with nitrogen for 15 min and then treated with 10 mg of $FeSO_4 \cdot 7H_2O$ and 1.2 mL of concentrated hydrochloric acid. The stream of nitrogen was continued for about 20 min for agitation, during which time the brown-colored solution gradually turned pink. The mixture was diluted with 80 mL of dichloromethane and washed with aqueous sodium acetate (30 mL, 10%) and then with water (2 × 50 mL). The solvent was evaporated; the residue was redissolved in 30 mL of diethyl ether and treated with an excess of distilled etheral diazomethane at room temperature. After 5 min, the solution was purged with nitrogen for 10 min and then evaporated. The crude product was chromatographed on a preparative TLC plate developed with methanol (1%)/dichloromethane. Three red bands, from top to bottom with a ratio of 1:5:3, were separated. The slowest moving band was identified as porphyrin *o* dimethyl ester **1b**, the middle band was found to be the acetylation derivative **2**, and the front moving band, with a diffuse band shape, much like that of protoporphyrin dimethyl ester on TLC plate, proved to be the dehydration product **3**. The combined yield of the three compounds was about 80%.

Dimethyl 2,7,12,18-Tetramethyl-3-[(4*E*,8*E*)-1-hydroxy-5,9,13-trimethyltetradeca-4,8,12-trienyl]-8-vinylporphine-13,17-dipropionate (1b). ^1H NMR: δ 11.02, 10.91, 10.53, 10.47 (s, 1 H each, meso H), 8.10 (m, 1 H, C*H*=CH_2), 6.35 (m, 2 H, vinyl CH=CH_2), −1.78 (d br, 2 H, NH); other substituents, see Table III. MS: *m/z* 813 (M + 1, 32%), 591 (M − farnesyl, 20%). IR: ν = 3314 cm^{-1} (br), 2957, 2924, 2851, 1738, 1666, 1506, 1456, 1437, 1377, 1346, 1259, 1196, 1169, 1097, 1022, 910, 835, 802, 734, 679. UV–vis: λ (rel intens) 404 nm (1.00), 502 (0.09), 536 (0.07), 571 (0.05), 626 (0.03).

Dimethyl 2,7,12,18-Tetramethyl-3-[(4*E*,8*E*)-1-acetoxy-5,9,13-trimethyltetradeca-4,8,12-trienyl]-8-vinylporphine-13,17-dipropionate (2). ^1H NMR δ 10.93, 10.90, 10.53, 10.50 (s, 1 H each, meso H), 8.12 (dd, 1 H, C*H*=CH_2), 7.28 (m, 1 H, C*H*OAcCH_2), 6.34 (m, 2 H, vinyl CH=CH_2), −1.70 (t, br, 2 H, NH); other substituents, see Table III. MS: *m/z* 855 (M + 1, 32%), 795 (M − AcOH), 591 (M − farnesyl, 20%), −1.67 (dd, br, NH). IR: ν = 3312 cm^{-1}, 2955, 2924, 2855, 1738, 1624, 1523, 1437, 1639, 1259, 1234, 1197, 1169, 1080, 1020, 914, 800, 742, 679. UV–vis: λ (rel intens) 403 nm (1.00), 503 (0.09), 536 (0.07), 572 (0.05), 626 (0.03).

Dimethyl 2,7,12,18-Tetramethyl-3-[(2*E*,4*E*,8*E*)-5,9,13-trimethyltetradeca-2,4,8,12-tetraenyl]-8-vinylporphine-13,17-dipropionate (3). ^1H NMR ($CDCl_3$): δ 10.56, 10.53, 10.24, 10.14, (s, 1 H each, meso H), 8.10 (m, 1 H, C*H*=CH_2), 7.80 (d, 1 H each, C*H*=CH), 6.77 (sextet, 1 H, CH=C*H*), 6.37 (m, 2 H, vinyl CH=CH_2), −1.85 (s, br, 2 H, NH); other substituents, see Table III. MS: *m/z* 795 (M + 1, 19%). IR: ν = 3314 cm^{-1}, 2957, 2924, 2870, 2855, 2727, 1738, 1601, 1458, 1377, 1261, 1197, 1169, 1101, 1078, 1022, 970, 902, 833, 802, 731, 677. UV–vis: λ (rel intens) 405 nm (1.00), 505 (0.09), 540 (0.07), 574 (0.05), 629 (0.03).

Results and Discussion

1. Preparation of the Iron-Free Porphyrin *o*. The paramagnetic nature of the extracted heme *o* precluded detailed NMR studies of the porphyrin macrocyclic structure. An attempt to prepare a diamagnetic bispyridine hemochrome sample was not successful because this particular batch of material did not undergo autoreduction in deuterated pyridine, as has been reported with heme *a*.[13] Owing to the scarcity of the amount of sample available, which severely limited our exploratory search for a suitable reducing system, it was decided that NMR characterizations be carried out by using the free base form of this heme. Demetalation of heme *o* was accomplished by a standard procedure using $FeSO_4$ in acidic medium,[11b] which had also been tested in our laboratory previously in preparing porphyrin *a*. This procedure successfully removed the metal ion, and the resultant free base porphyrins were first esterified by using diazomethane before chromatographic purification on preparative silica gel plates. Three major porphyrin fractions were obtained, and after a careful analysis on the spectroscopic data collected on each compound (vide infra), structure **1b** was assigned to heme *o* free base (i.e., porphyrin *o*) dimethyl ester, structure **2** to its acetylation derivative, and **3** to its dehydration derivative, respectively. For the purpose of comparison, three model compounds, **4**–**6**, were also prepared according to literature procedures.[10,12] Compound **4** is the core structure of **1b**, and compound **5** is the regioisomer of **4** with the positions of the α-hydoxyethyl and vinyl substituents reversed. Compound **6** possesses the core structure of heme *a* with the vinyl and formyl group diagonally seated. The spectroscopic data analysis on these novel structures is described in the following sections.

(7) Puustinen, A.; Finel, M.; Haltia, T.; Gennis, R. B.; Wikström, M. *Biochemistry* **1991**, *30*, 3936–3942.
(8) Puustinen, A.; Wikström, M. *Proc. Natl. Acad. Sci. U.S.A.* **1991**, *88*, 6122–6126.
(9) (a) Varotsis, C.; Oertling, W.; Babcock, G. T. *Appl. Spectrosc.* **1990**, *44*, 742–744. (b) Babcock, G. T.; Vickery, L. E.; Palmer, G. *J. Biol. Chem.* **1976**, *251*, 7907–7919.
(10) Clezy, P. S.; Fookes, C. J. R.; Hai, T. T. *Aust. J. Chem.* **1978**, *31*, 365–379.
(11) (a) Falk, J. *Porphyrins and Metalloporphyrins*; Elsevier/North-Holland: New York, 1964; pp 133–135. (b) *Ibid.* pp 132–133. (c) *Ibid.* pp 72–80.
(12) Chang, C. K.; Hatada, M. H.; Tulinsky, A. *J. Chem. Soc., Perkin Trans. 2* **1983**, *371*.
(13) Caughey, W. S.; Smythe, G. A.; O'Keefe, D. H.; Maskasky, J. E.; Smith, M. L. *J. Biol. Chem.* **1975**, *250*, 7602–7622.

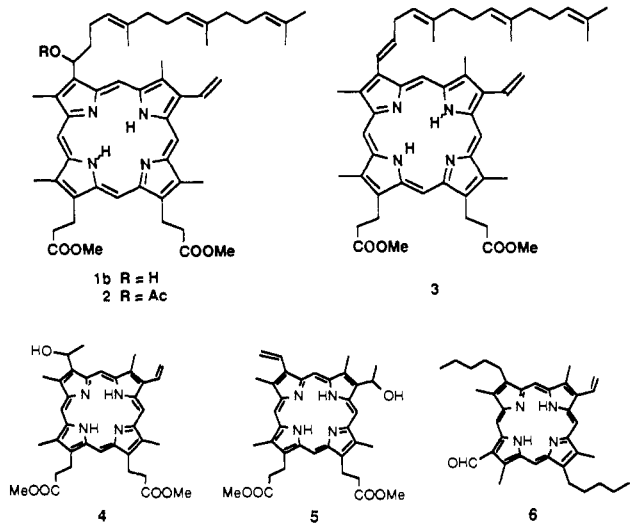

2. Mass Spectra. Fast atom bombardment mass spectrometry yielded a mass of 838.5 for the iron(III) heme *o* moiety **1a** ($C_{49}H_{58}N_4O_5Fe$ requires 838.4), which is smaller to that of 839 reported by the Helsinki group.[8] The metal free porphyrin *o* dimethyl ester **1b** gave a satisfying M + 1 peak at 813.5000 ($C_{51}H_{65}N_4O_5$ requires 812.4955) corresponding to the removal of iron and addition of the two methyl ester groups to the macrocycle. A fragment with a mass of 591 indicates the loss of the homo-farnesyl side chain through the cleavage of the 1,2-C–C bond next to the oxygen atom to yield a porphyrin—C^+=O ion. A mass of 565 peak is also present and assignable to an ion resulting from cleavage of the entire farnesylethyl substituent. Compound **2** gave a mass spectrum with a $[M + 1]^+$ ion of 855 that corresponds to the replacement of the HO– group by a CH_3COO– group. A fragment peak at 795 represents the loss of a CH_3COOH moiety, and a 591 ion again results from the cleavage of the homo-farnesyl side chain as well as the acetyl group. Compound **3** has a prominent $[M + 1]^+$ ion of 795 which is 18 units smaller than that of **1b**, indicating the dehydration of the secondary alcohol. Both compounds **2** and **3** are derived from heme *o* **1a** during the process of demetalation since the ^1H NMR spectra of the crude mixture of porphyrin *o* dimethyl ester prior to chromatographic separation exhibit multiple peaks in the meso protons region corresponding to the three porphyrins.

3. Vibrational Spectra. a. Infrared Spectra. Heme *a* has a prominent band at 1667 cm^{-1}, and model compound **6** has a band at 1661 cm^{-1} that arises from the formyl carbonyl stretching vibrations.[13,18] No such band is observed in the spectra of heme *o* **1a** and porphyrin **1b**, **2**, and **3**, thereby excluding the presence of a formyl group in these compounds. While the inner N–H groups of the metal-free porphyrins absorb near 3315 cm^{-1} as weak but relatively sharp bands, the O–H stretching bands of the *a*-hydroxy on the farnesylethyl side chain of heme *a* and porphyrin *o* **1b** appear at higher wavenumbers and are significantly broader. The out-of-plane C–H bending vibrations of the vinyl group of porphyrin *o* are observed at 903 and 970 cm^{-1} for $=CH_2$ and CH=, respectively. These bands are characteristic vibrational modes for vinyl groups attached to the porphyrin ring and are usually strong in the olefin fingerprint region between 1000 and 650 cm^{-1}.[14,15] A prominent band at 802 cm^{-1}, which appears in the spectra of all porphyrins bearing a farnesyl side chain, is attributed to the bending vibration mode of the C–H bond on the trisubstituted unconjugated olefin. This band is seen in the spectra of heme, *a*, porphyrin *o* dimethyl ester **1b**, and its derivatives **2** and **3**, but is absent from that of protoporphyrin as well as from those of model compounds **4–6** that have no farnesyl side chain attached.

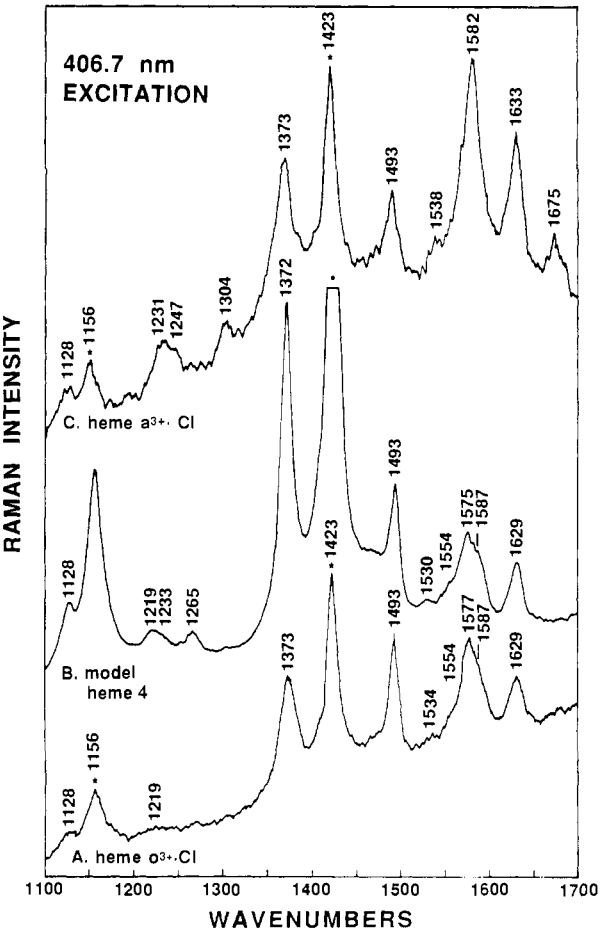

Figure 1. Resonance Raman spectra of (A) heme *o*, (B) Fe(III)·Cl of porphyrin **4**, and (C) heme *a* iron(III) chloride. The excitation wavelength was at 406.7 nm, and the measurements were carried out at room temperature in CH_2Cl_2 solution.

Table I. Resonance Raman Frequencies (cm^{-1}) of Heme *o* and Other Porphyrin Models above 1100 cm^{-1}

mode	heme *o*·chloride	4–Fe·Cl	5–Fe·Cl	heme *a*·chloride	PPFe·Cl[a]
$\nu(C_b—C_a)$	1128	1128	1128	1128	1130
$\nu_2(C_b—C_b)$	1577 A_{1g}	1575	1575	1582	1570
$\nu_3(C_a—C_m)$	1493 A_{1g}	1493	1493	1493	1491
$\nu_4(C_a—N)$	1373 A_{1g}	1372	1372	1373	1373
$\nu_{10}(C_a—C_m)$	1629 B_{1g}	1629	1629	1633	1626
$\nu(C=C)$	1622	1622	1622		1626
$\nu_{37}(C_b—C_b)$	1586 E_u	1587	1587		1591
$\nu(C=O)$				1675	
$\nu_{13}\delta(C_m—H)$	1219	1219	1219		1228
$\nu_5 + \nu_9$	1265	1265	1265		1260
$\nu_{11}(C_b—C_b)$	1534	1530	1530	1538	1533
	1554	1554	1554		1553

[a] PPFe·Cl = protohemin chloride.

b. Resonance Raman Spectra. Representative resonance Raman spectra of the chloride complexes of ferric heme *o* and of model porphyrin **4**, with Fe(III) incorporated are shown in Figure 1. The excitation wavelength, 406.7 nm, is near the maximum of the B(0,0) absorption band. For comparison, the spectrum of heme *a* is also shown. The observed RR bands are assignable to fundamental porphyrin skeletal modes of heme *o* and of the relevent porphyrin model compounds and are summarized in Table I. The modes are numbered according to the scheme used by Abe et al. for NiOEP.[16] The frequencies of the corresponding skeletal vibrations of the chloride complexes of ferric heme *a* and protoheme are also given in Table I. All but a few of the RR

(14) Caughey, W. S.; Alben, J. O.; Fujimoto, W. Y.; York, J. L. *J. Org. Chem.* **1966**, *31*, 2631.
(15) Boucher, L. J.; Katz, J. J. *J. Am. Chem. Soc.* **1967**, *89*, 1340.
(16) Abe, M.; Kitagawa, T.; Kyogoku, Y. *J. Chem. Phys.* **1978**, *69*, 4526–5534.

Table II. UV–Visible Absorption Maxima of Porphyrins in CH_2Cl_2 (Wavelength, nm)

compd	band I	band II	band III	band IV	Soret
1b	626	571	536	502	404
2	626	572	536	503	403
3	629	574	540	505	405
4	625	571	536	502	403
5	625	571	536	502	403
6	634	377	557	515	413
P*a*DME[a]	647	584	560	517	412
PPDME[a]	629	575	540	505	406

[a] P*a*DME = porphyrin *a* dimethyl ester; PPDME = protoporphyrin dimethyl ester.

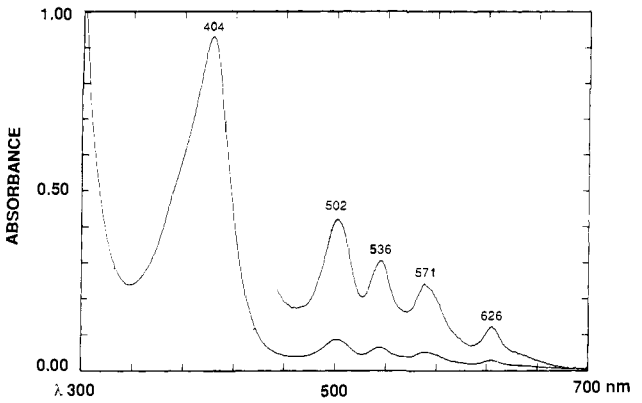

Figure 2. Visible absorption spectrum of porphyrin *o* dimethyl ester (**1b**), in CH_2Cl_2.

vibrations of the heme *o* and its model compounds are within 2 cm^{-1} of the analogous bands of heme *a* and protoheme,[17a] the clear exceptions being ν_2 and ν_{11}. These modes involve substantial C_b–C_b motion and are sensitive to the identity and pattern of substitution at the periphery of the macrocycle. Variation in the frequency of these modes with the identity of the porphyrins is expected. Relative to heme *a*, heme *o* and its model also show strong enhancement of the ν_{37} mode (1586 cm^{-1}), which probably reflects symmetry lowering effects, and more importantly, the absence of a mode attributable to a peripheral formyl group. The occurrence of a vinyl substituent in heme *o* is supported by the appearance of a mode at 1622 cm^{-1} that is assigned to the C=C stretching motion. Like other iron porphyrin macrocycles, the ring skeletal modes of heme *o* are sensitive to iron spin, coordination, and valence states. A complete analysis of this dependence will be presented elsewhere.[17b]

4. Electronic Absorption Spectra. The visible spectral data collected from porphyrin *o* dimethyl ester and related compounds are listed in Table II. Porphyrin **1b** (the spectrum of which is shown in Figure 2) and its acetylation derivative **2** have UV–visible spectra very similar to those of their model compounds **4** and **5**, thus strongly arguing that they have a common aromatic macrocycle with the same auxochrome groups attached. Similar to what was observed in the pyridine hemochrome spectrum of its iron complex,[8] the visible bands of **1b** are 3–4 nm blue shifted and the Soret band is 2 nm blue shifted from those of protoporphyrin IX dimethyl ester. This provides further evidence that only one vinyl group is present in porphyrin *o*. Interestingly, when **1b** undergoes dehydration to generate a new double bond conjugating with the macrocycle, i.e., compound **3**, the visible spectrum obtained is indistinguishable from that of protoporphyrin. Unlike porphyrin *a*, which has a unique oxo–rhodo-type visible band due to its "rhodofying groups" (vinyl and formyl occupying opposite pyrrolic rings, i.e., on positions 8 and 18) in the macrocycle, porphyrin *o* gives, like that of protoporphyrin, an etio-type visible absorption.[11c] This means that the rhodofying effect is missing and that the farnesyl group does not have a significant influence on the visible absorption pattern.

(17) (a) Callahan, P. M.; Babcock, G. T. *Biochemistry* **1981**, *20*, 952–958. (b) Varotsis, C.; Babcock, G. T.; Wu, W.; Chang, C. K.; Puustinen, A.; Wikström, M. Manuscript in preparation. The ν(C=C) vibration at 1622 cm^{-1} is obscured by ν_{10} in Figure 1 but becomes clear in spectra taken with different polarization.

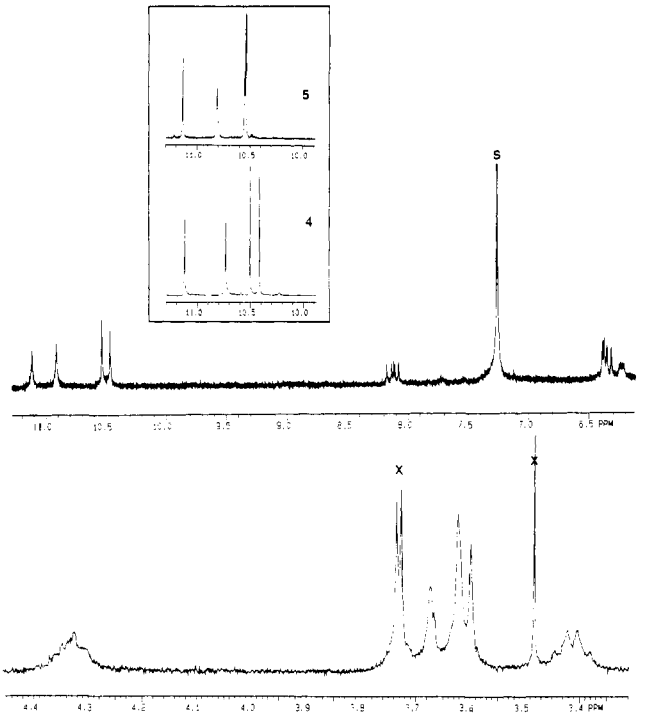

Figure 3. ^1H NMR spectra (in $CDCl_3$, 300 MHz) of porphyrin *o* dimethyl ester (**1b**); the peaks at 3.48, 3.73, and 3.74 ppm were from impurities as verified by synthetic **1b** (unpublished results). Inset: spectra of the meso protons of model porphyrins **4** and **5**.

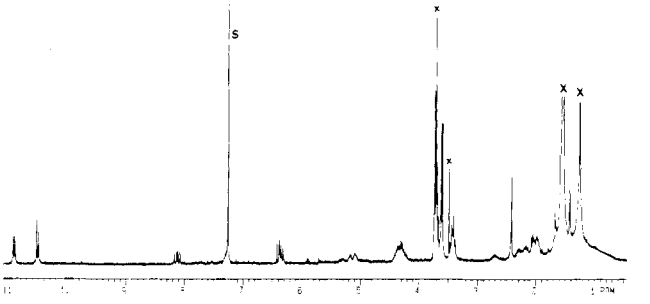

Figure 4. ^1H NMR spectrum (in $CDCl_3$, 300 MHz) of **2**.

5. Nuclear Magnetic Resonance Spectra. Owing to the submilligrams of samples available, a large number of transients, 7000–10000 scans, had to be applied to collect each ^1H NMR spectrum. In the high-purity deuterated chloroform solvent employed, the sample porphyrins were protonated by the trace amount of HCl commonly present in the solvent, as evidenced by the formation of a pink-colored solution instead of the typical brown-red color. The observed chemical shifts of the meso protons were shifted downfield because of this protonation. The spectrum of **1b** is presented in two segments in Figure 3, and the full spectrum of **2** is given in Figure 4.

The ^1H NMR assignments for **1b** are clearly consistent with the presence of four meso protons, four ring methyls, two methyl propionate side chains, and a vinyl group as required by the structure proposed. However, the signals of the farnesyl side chain are not so well distinguished. That there is no formyl group in **1b** is immediately evident since no additional H—C=O proton resonance was observed in the 11–12 ppm region. The chemical shifts in the downfield region in the spectra of porphyrin *o* dimethyl ester **1b** and its acetylation derivative **2**, in comparison with model compounds **4** and **5** in their protonated forms, are listed in Table III. The well-matched meso proton positions of **1b** and **4** (Figure 3 inset) indicate that these two compounds should have the same

Table III. Chemical Shifts (ppm) of Porphyrin *o* and Other Model Porphyrins (in $CDCl_3$)

assignments		1b	2	3	4	5
meso proton	5	11.02 (s)	10.93 (s)	10.56 (s)	11.20 (s)	10.55 (s)
	10	10.53 (s)	10.53 (s)	10.53 (s)	10.54 (s)	11.14 (s)
	15	10.91 (s)	10.90 (s)	10.24 (s)	10.79 (s)	10.82 (s)
	20	10.47 (s)	10.50 (s)	10.14 (s)	10.47 (s)	10.54 (s)
vinyl		8.10 (dd)	8.12 (dd)	8.10 (m)	8.14 (dd)	8.14 (dd)
		6.33 (dd)	6.34 (dd)	6.37 (m)	6.35 (dd)	6.36 (dd)
methyl propionate		4.33 (t)	4.32 (t)	4.30 (t)	4.41 (t)	4.41 (t)
		3.42 (t)	3.44 (t)	3.29 (t)	3.17 (t)	3.18 (t)
		3.40 (t)	3.40 (t)	3.29 (t)	3.16 (t)	3.16 (t)
		3.62 (s)	3.62 (s)	3.65 (s)	3.62 (s)	3.62 (s)
		3.62 (s)	3.62 (s)	3.65 (s)	3.61 (s)	3.61 (s)
ring methyl	2	3.66 (s)	3.69 (s)	3.60 (s)	3.54 (s)	3.63 (s)
	7	3.67 (s)	3.69 (s)	3.70 (s)	3.63 (s)	3.53 (s)
	12, 18	3.60	3.60 (s)	3.65	3.57 (s)	3.57 (s)
		3.62	3.62	3.66 (s)	3.59 (s)	3.59 (s)
farnesylethyl	1′	6.40 (t)	7.28	7.80 (d, J = 16 Hz)		
(H or CH_3)	2′	2.10–2.70	2.10–2.70	6.77 (sextet)		
	3′	2.10–2.70	2.10–2.70	1.96–2.30		
	4′	5.40	5.35	5.05–5.40		
	5′	1.68	1.68	1.69		
	6′	1.90–2.30	1.90–2.30	1.90–2.30		
	7′	1.90–2.30	1.90–2.30	1.90–2.30		
	8′	5.15	5.18	5.05–5.40		
	9′	1.62	1.68	1.69		
	10′	1.90–2.30	1.90–2.30	1.90–2.30		
	11′	1.90–2.30	1.90–2.30	1.90–2.30		
	12′	5.10	5.09	5.05–5.40		
	13′	1.60, 1.61	1.60, 1.62	1.62, 1.63		

pattern of substituent arrangement on the macrocycle, that is, two methyl propionate side chains at positions 13 and 17, the farnesylethyl group of porphyrin *o* at position 3, and a vinyl group at position 8. This arrangement is further reinforced by observing appropriate nuclear Overhauser enhancements (NOE), which reveal the position of the individual meso protons along with their proximity to different side chains. For example, irradiation of the 8-vinyl group (8.10 ppm) gave NOE at the 7-methyl (3.67 ppm) and meso 10-protons (10.53 ppm). Irradiation of the 7-methyl then yielded NOE on the meso 5-proton (11.02 ppm), which in turn affected the hydroxy-substituted side chain. Had the position of the farnesylhydroxyethyl group and the vinyl group been transposed, a different set of connectivities would be observed. These assignments are also viable on the basis of the established pattern of porphyrin biosynthesis in which one of the two vinyl groups of protoporphyrin might be modified. Considering the possible biosynthetic relationship between heme *o* and heme *a*, a similar arrangement of the peripheral substituents is certainly anticipated. In the spectrum of compound **2**, the CH_3 of an acetyl group is seen as a sharp resonance at 2.41 ppm. In the spectrum of **3**, the two protons on the α–β double bond formed after dehydration are located at 7.80 and 6.77 ppm, respectively. The 16-Hz coupling constant detected strongly supports a trans configuration. The formation of the acetylation derivative **2** and the dehydration product **3** lends further support for the correct assignment of the α-hydroxy-substituted farnesylethyl side chain. Owing to the necessary high dilution conditions under which these samples were measured, it was unavoidable that some peaks were buried under impurity peaks, particularly those of the farnesyl side chain for which individual assignments have been difficult to determine. Nevertheless, in comparison with the ^1H NMR data obtained from porphyrin *a*,[13,18,19] as well as from model compounds, it has been possible to make assignments for the entire molecule without serious ambiguity.

6. Comparisons between Heme *o* and Heme *a*. From the sum of the experiments presented above, the structure **1b** is now established for porphyrin *o* dimethyl ester. There can be little doubt that the parent heme *o*, the iron complex of this macrocycle without the ester (structure **1a**), must also bear the same functional groups and substitution pattern given the spectroscopic evidence described above for the unmodified heme *o* itself. The final proof will come from a total synthesis of porphyrin *o* into which iron is inserted, followed by comparison with the naturally occurring prosthetic group; this effort is currently underway.

With the establishment of the heme *o* structure, the similarities between the quinol-oxidizing cytochrome *o* system and the cytochrome-oxidizing cytochrome aa_3 enzymes are even more striking. Both possess the heme/Cu_B binuclear center at which O_2 reduction to water occurs and a low-spin heme iron that is involved in transferring electrons from the reducing substrate to the binuclear center. A unique feature of heme *a* is that the formyl group increases its redox potential relative to protoheme; a higher potential of the prosthetic group is consistent with the sequence of electron transfers in mitochondrial respiration. An apparently important aspect of the function of heme *a* based terminal oxidase is the delicate tuning of the redox potential interaction between the iron and copper redox centers in the enzyme.[18] Recent experiments by Salerno and co-workers[3] have established that similar potentials and redox interactions occur in the heme *o* based quinol oxidases. As heme *o* has been shown here to lack the peripheral formyl group, these observations suggest that, in the heme *o* quinol oxidases, local protein effects are in force that modify the potential of the prosthetic groups to compensate for the absence of the formyl. The structural basis for redox potential modulation in the quinol oxidases may be apparent in primary sequence differences between the quinol and cytochrome oxidases.

It would be useful at this stage to comment on some of the minor disparities between the two porphyrin ligands. The difference in inherent redox potentials expected for the two prosthetic groups has already been commented upon. It has been reported that porphyrin *a* dimethyl ester is extremely photolabile.[19] Porphyrin *o* seems to be more stable to light as judged by its behavior on TLC plates and in methylene chloride or chloroform solution in normal room light. The stability could attribute to the absence of the 18-formyl group that might have activated the porphyrin toward photoinduced reactions. The absence of the electron-withdrawing formyl group might have other effects on the chemistry of the macrocycle. Battersby[20] has pointed out that

(18) (a) Wikström, M.; Krab, K.; Saraste, M. *Cytochrome Oxidase, a Synthesis*; Academic Press: New York, 1981. (b) Moody, J. A.; Rich, P. R. *Biochim. Biophys. Acta* **1990**, *205*, 1015.

(19) Battersby, A. R.; McDonald, E.; Thompson, M. *J. Chem. Soc., Perkin Trans 1* **1985**, 135–143.

(20) Battersby, A. R.; Cardwell, K. S.; Leeper, F. J. *J. Chem. Soc., Perkin Trans 1* **1986**, 1565–1580.

racemization of the chiral center, the secondary alcohol at the point of attachment of the farnesylethyl side chain to the macrocycle of heme *a*, can occur under acidic conditions and possibly under basic conditions also, and this is due to the electron-withdrawing effect of the formyl group. Whether there is racemization of the porphyrin *o* chiral center during the preparation process is not known at this stage, but the dehydration of the secondary alcohol that happened with porphyrin *o* appears to be more facile than expected. The replacement of the formyl group with a methyl group at position 18 would certainly decrease the acidity of the α-proton of the secondary alcohol, and might thus lead only to the elimination of a β-proton in the form of dehydration.

The farnesyl group present in heme *a* and heme *o* may have important roles for both hemes in their biological functions about which we can only speculate. One possible role of this side chain is to act as a lipophilic anchor holding the heme in the proper position within the membrane protein. Such a role for a hydrophobic tail appears to occur for the chlorophyll side chain in the photosynthetic reaction center.[21] Other roles could be related to electron transfer.[13] Woodruff et al.[22] recently proposed that one of the unsaturated isoprenoid groups of the farnesyl chain might alternatively coordinate heme iron and the nearby Cu ion in aa_3-type cytochrome *c* oxidases, and that such coordination might play a significant role in redox-linked proton translocation. The finding by Puustinen et al[23] that the cytochrome *o* oxidase is also proton-translocating is consistent with this idea. Considering the close structural resemblance between these hemes, it is possible that they are related in biosynthesis. Very few studies on the biosynthesis of heme *a* are recorded in the literature, but it is generally believed that protoporphyrin IX is the biogenetic precursor.[24] A likely mechanism for formation of the side chain at C-3 that uses farnesyl pyrophosphate has been proposed.[25] Clezy and Fookes[26] reported a decade ago the synthesis of **1b** as a possible precursor of heme *a*. At that time it was not realized that **1a** itself is a prosthetic group of a natural quinol oxidase. Even now, we are not certain if porphyrin *o* is indeed an intermediate in the biosynthetic pathway of heme *a*, that is, whether it lies between protoporphyrin and porphyrin *a*. This seems to be a worthwhile objective to pursue in the future.

Acknowledgment. This work was supported by the NIH Grants GM 34468 and 36520 (C.K.C.) and GM 25480 (G.T.B.), the Sigrid Jusèlius Foundation, and the Academy of Finland (M.W.). The NMR data were obtained on instrumentation purchased in part with funds from NIH Grant 1-S10-RR04750-01 and from NSF Grant CHE 88-00770.

(21) Michel, H.; Diesenhofer, J. *Biochemistry* **1988**, *27*, 1.
(22) Woodruff, W. H.; Einarsdóttir, Ó.; Dyer, R. B.; Bagley, K. A.; Palmer, G.: Atherton, S. J.; Goldbeck, R. A.; Dawes, T. D.; Kliger, D. S. *Proc. Natl. Acad. Sci. U.S.A.* **1991**, *88*, 2588-2592.
(23) Puustinen, A.; Finel, M.; Virkki, M.; Wikström, M. *FEBS Lett.* **1989**, *249*, 163-167.
(24) Weinstein, J. D.; Branchaud, R.; Beale, S. I.; Bement, W. J.; Sinclair, P. R. *Arch. Biochem. Biophys.* **1986**, *245*, 44.
(25) Leeper, F. J. *Nat. Prod. Rep.* **1985**, *2*, 19-47.
(26) Clezy, P. S.; Fookes, C. J. R. *Aust. J. Chem.* **1981**, *34*, 871-883.

Spectroscopic Studies of *p*-(*N*,*N*-Dimethylamino)benzonitrile and Ethyl *p*-(*N*,*N*-Dimethylamino)benzoate in Supercritical Trifluoromethane, Carbon Dioxide, and Ethane

Ya-Ping Sun,[†] Marye Anne Fox,*[,†] and Keith P. Johnston*[,‡]

Contribution from the Departments of Chemistry and Chemical Engineering, The University of Texas at Austin, Austin, Texas 78712. *Received July 29, 1991*

Abstract: Absorption and emission spectral maxima, bandwidths, and fractional contribution of twisted intramolecular charge transfer states to the observed emission of *p*-(*N*,*N*-dimethylamino)benzonitrile (DMABN) and ethyl *p*-(*N*,*N*-dimethylamino)benzoate (DMAEB) in supercritical CHF_3, CO_2, and C_2H_6 are presented. By examining a wide range of reduced densities from 0.05 to 2.2, we have discovered a characteristic density dependence in the spectral shifts in all three fluids. A model for these spectral effects is proposed, differentiating intermolecular interactions in three distinct regions: gas-phase solute–solvent clustering, clustering in the near-critical region, and "liquidlike" solvation. Even below a reduced density of 0.5, clustering of solvent about solute is already prevalent.

Introduction

Molecular spectroscopy in supercritical fluids is a relatively new research subject, since the utility of this medium in probing solvent effects on photophysical phenomena has only recently been recognized.[1-11] Solvent friction, polarity, and clustering effects, which are very important in this regard both experimentally and theoretically,[12-14] are particularly amenable to study in supercritical fluids. The unique feature of a supercritical fluid is that its solvation properties can be continuously varied over a wide range, making it possible to probe solute–medium interactions without changing solvent. The density of a supercritical fluid is lower than the bulk density of the liquid phase, but larger than what is usually encountered in clusters in a supersonic jet expansion. Spectroscopic studies in supercritical fluids of various solute probes can therefore

[†] Department of Chemistry.
[‡] Department of Chemical Engineering.

(1) Okada, T.; Kobajashi, Y.; Yamasa, H.; Mataga, N. *Chem. Phys. Lett.* **1986**, *128*, 583.
(2) Kim, S.; Johnston, K. P. *Ind. Eng. Chem. Res.* **1987**, *26*, 1206.
(3) Kim, S.; Johnston, K. P. *AIChE J.* **1987**, *33*, 1603.
(4) Kajimoto, O.; Futakami, M.; Kobayashi, T.; Yamasaki, K. *J. Phys. Chem.* **1988**, *92*, 1347.
(5) Yonker, C. R.; Smith, R. D. *J. Phys. Chem.* **1988**, *92*, 235.
(6) Hrnjez, B. J.; Yazdi, P. T.; Fox, M. A.; Johnston, K. P. *J. Am. Chem. Soc.* **1989**, *111*, 1915.
(7) Brennecke, J. F.; Eckert, C. A. *Am. Chem. Soc. Symp. Ser.* **1989**, *406*, 14. Brennecke, J. F.; Tomasko, D. L.; Peshkin, J.; Eckert, C. A. *Ind. Eng. Chem. Res.* **1990**, *29*, 1682.
(8) Johnston, K. P.; Kim, S.; Combes, J. *Am. Chem. Soc. Symp. Ser.* **1989**, *406*, 52.

0002-7863/92/1514-1187$03.00/0